

TECHNICAL NOTE

## A non-linear elastic/perfectly plastic analysis for plane strain undrained expansion tests

M. D. BOLTON\* and R. W. WHITTLE†

**KEYWORDS:** elasticity; pore pressures; shear strength; stiffness.

INTRODUCTION

This note presents the solution for the undrained expansion of a cylindrical cavity in a non-linear elastic/perfectly plastic soil, using a power law characteristic to describe the decay of stiffness with strain.

Two additional soil parameters are required to implement the solution, a stiffness constant  $\alpha$  and an elastic exponent  $\beta$ . Both parameters are obtained from pressuremeter tests incorporating cycles of unloading and reloading.

A typical undrained self-bored pressuremeter test with unload/reload cycles is shown in Fig. 1. This test will be used as an example throughout the following text. The curvature of the initial part of the expansion and the unload/reload cycles show the elastic response of the ground is non-linear, becoming less stiff with increasing strain. Nevertheless, it is common practice to reduce such data to fundamental strength and stiffness properties using analyses that assume the ground response to loading is simple elastic/perfectly plastic. The solution presented in this note is a small step in the direction of more realistic soil models. Even so, it is capable of explaining much that has been puzzling users of pressuremeter data.

Figure 2 gives the idealized shear stress versus shear strain response for the loading of a non-linear elastic/perfectly plastic soil. The shear strain when a fully plastic response is achieved is denoted  $\gamma_y$ , and at this strain there is a corresponding secant shear modulus  $G_y$ , which is a minimum value. At shear strains smaller than  $\gamma_y$  the secant shear modulus is higher than  $G_y$ .

A power law function is often found to fit data of reducing stiffness with strain (Gunn, 1992; Bolton *et al.*, 1993), so the variation of shear stress with strain shown in Fig. 2 can be written

$$\tau = \alpha\gamma^\beta \tag{1}$$

where  $\alpha$  and  $\beta$  must be discovered. It will be demonstrated later that this equation gives a satisfactory fit to field data and leads to a closed form solution for the undrained loading of a cylindrical cavity, the problem posed by a pressuremeter test.

THE NON-LINEAR ELASTIC/PERFECTLY PLASTIC SOLUTION

Around the pressuremeter, assume that the soil is deformed under conditions of axial symmetry and the expansion is undrained. Fig. 3 shows the essential pressures and displacements, and the following relationships apply: axial strain  $\epsilon_a = 0$ ; circumferential strain  $\epsilon_\theta = -\rho/r$ ; the expansion is undrained, so  $\epsilon_v = 0$  and radial strain  $\epsilon_r = -\epsilon_\theta = \rho/r$ ; shear strain  $\gamma = \epsilon_r - \epsilon_\theta = 2\rho/r = \delta A/A$  at the cavity wall. The equation of radial equilibrium applies throughout the expansion:

$$r \frac{d\sigma_r}{dr} + (\sigma_r - \sigma_\theta) = 0 \tag{2}$$

where  $\sigma_r$  is radial stress and  $\sigma_\theta$  is circumferential stress.

*Elastic loading*

Using  $\tau$  to represent the maximum shear stress, equation (2) becomes

$$r \frac{d\sigma_r}{dr} + 2\tau = 0 \tag{3}$$

Now using the constitutive relationship  $\tau = \alpha\gamma^\beta$  given by equation (1) and writing the current area in terms of radius:

$$\frac{d\sigma_r}{dr} + \frac{2\alpha}{r} \left( \frac{\delta A}{\pi r^2} \right)^\beta = 0 \tag{4}$$

Noting that  $(1/r)(1/r^2)^\beta = r^{-(2\beta+1)}$ :

Manuscript received 23 December 1996; revised manuscript accepted 19 August 1998.

Discussion on this technical note closes 7 May 1999; for further details see p. ii.

\* University of Cambridge.

† Cambridge Insitu.

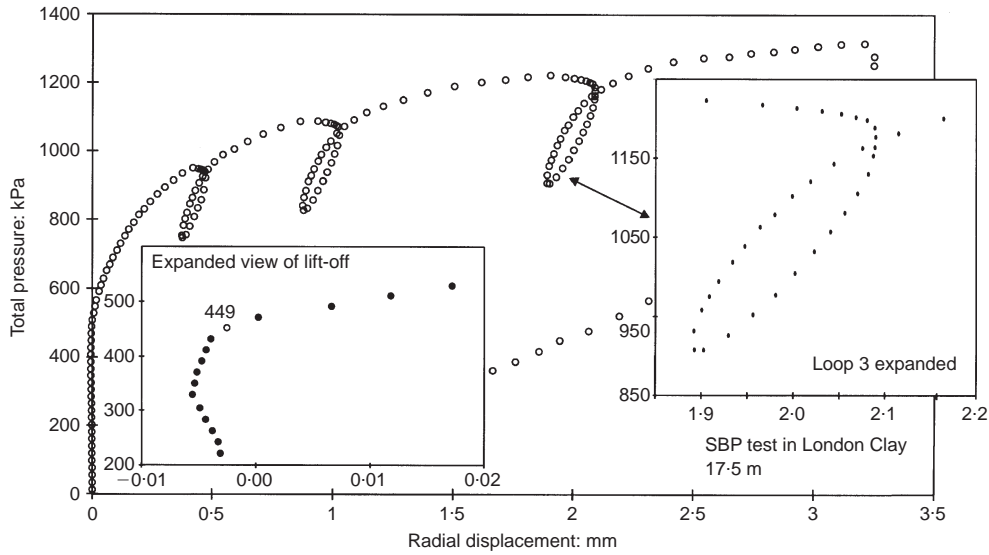


Fig. 1. A self-bored pressuremeter test with three unload/reload cycles

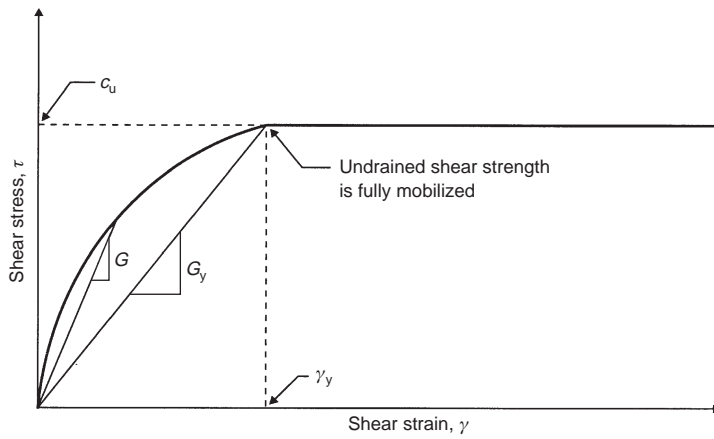


Fig. 2. Shear stress: shear strain response for ideal non-linear elastic/perfectly plastic soil

$$\frac{d\sigma_r}{dr} + 2a \left( \frac{\delta A}{\pi} \right)^\beta r^{-(2\beta+1)} = 0 \quad (5)$$

The pressuremeter provides data for changes in radius  $r_c$  and radial stress  $p_c$  measured at the cavity wall. At infinite radius from the pressuremeter the stress acting will be the reference stress  $p_0$ , so integrating between this reference condition, and the pressure and radius at the cavity wall:

$$[\sigma_r]_{p_0}^{p_c} = -2a \left( \frac{\delta A}{\pi} \right)^\beta \int_{\infty}^{r_c} r^{-(2\beta+1)} dr \quad (6)$$

so

$$p_c - p_0 = 2a \left( \frac{\delta A}{\pi} \right)^\beta \left( \frac{1}{r^2} \right)^\beta \left( \frac{1}{2\beta} \right) = \frac{a}{\beta} \left( \frac{\delta A}{A} \right)^\beta \quad (7)$$

Now applying equation (1) at the cavity boundary where  $r = r_c$  we can write

$$\tau_c = \alpha \left( \frac{\delta A}{A} \right)^\beta \quad (8)$$

This can be used in equation (7) to obtain

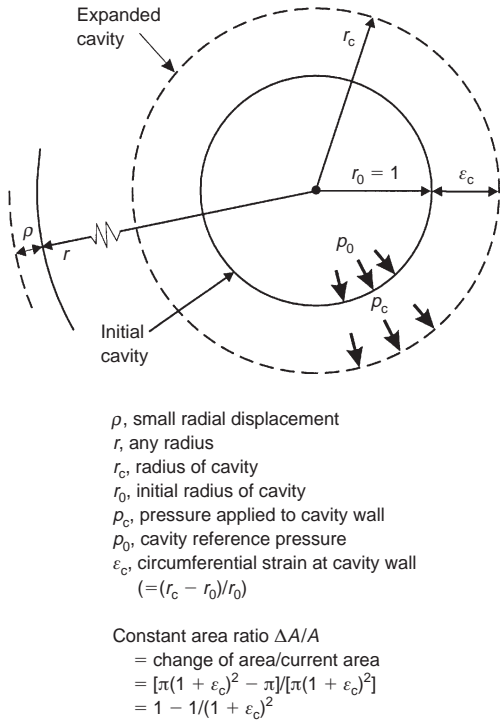


**Fig. 3. Pressures and displacements associated with the pressuremeter**

$$p_c - p_0 = \frac{\tau_c}{\beta} \quad (9)$$

The end of the elastic phase is reached when  $\tau_c = c_u$  and hence  $p_c - p_0 = c_u/\beta$ . The shear strain  $\Delta A/A$  at this point will be  $\gamma_y$ , shown in Fig. 2.

#### Plastic loading

Thereafter, as the expansion continues there is a plastic zone confined by the limiting elastic radial stress of  $c_u/\beta$ . The stress distribution around the pressuremeter is shown in Fig. 4.

Equation (3) still applies, so

$$r \frac{d\sigma_r}{dr} + 2c_u = 0 \quad (10)$$

This gives

$$d\sigma_r = -2c_u \frac{dr}{r} \quad (11)$$

Integrating between the radii of the cavity wall and of the elastic-plastic transition:

$$\int_{p_c}^{p_0 + c_u/\beta} d\sigma_r = -2c_u \int_{r_c}^{r_y} \frac{dr}{r}$$

Hence

$$p_c = p_0 + c_u \left[ \frac{1}{\beta} + \ln \left( \frac{r_y^2}{r_c^2} \right) \right] \quad (12)$$

In a soil being sheared at constant specific volume  $r_y^2/r_c^2 = \gamma_y/\gamma_c$  (Gibson & Anderson, 1961) leading to

$$p_c = p_0 + c_u \left[ \frac{1}{\beta} - \ln(\gamma_y) + \ln(\gamma_c) \right] \quad (13)$$

This result resembles the simple elastic/perfectly plastic solution proposed by Gibson & Anderson. For the special case of a simple elastic response when  $\beta = 1$  the two solutions are identical. Indefinite expansion of the borehole is predicted by

$$p_{\text{Limit}} = p_0 + c_u \left[ \frac{1}{\beta} - \ln(\gamma_y) \right] \quad (14)$$

and substituting this into equation (13) gives

$$p_c = p_{\text{Limit}} + c_u \ln(\gamma_c) \quad (15)$$

showing that the undrained shear strength and limit pressure can be obtained from the gradient and intercept of a plot of total pressure at the cavity wall versus the natural log of the current shear strain at the cavity wall.

#### OBTAINING $\alpha$ AND $\beta$

The assumption that the reduction of stiffness with strain throughout the elastic phase can be described by a power law function is justified by inspection of unload/reload data. If the reloading data from unload/reload cycles are plotted on axes of pressure versus shear strain using log scales, then a linear relationship is evident. The reversal point in the cycle is the origin for subsequent data. An example from the test shown in Fig. 1 is given in Fig. 5. All loops give similar results, well fitted by a linear function.

The exponential of the linear function shown in Fig. 5 is a power law of the form  $p_c = \eta \gamma_c^\beta$  where  $p_c$  and  $\gamma_c$  are the radial stress and shear strain at the cavity wall and  $\eta$  and  $\beta$  are the intercept and gradient of the log-log relationship. Before using this expression to quote a value for modulus, radial stress needs to be converted to shear stress. While the soil is responding elastically it follows from equation (9) that

$$\tau_c = \eta \beta \gamma_c^\beta \quad (16)$$

so the stiffness constant  $\alpha$  is given by  $\eta \beta$ . Note from equations (9) and (16) that secant shear modulus  $G_s$  is given by

$$G_s = \eta \beta \gamma_c^{\beta-1} = \alpha \gamma_c^{\beta-1} \quad (17)$$

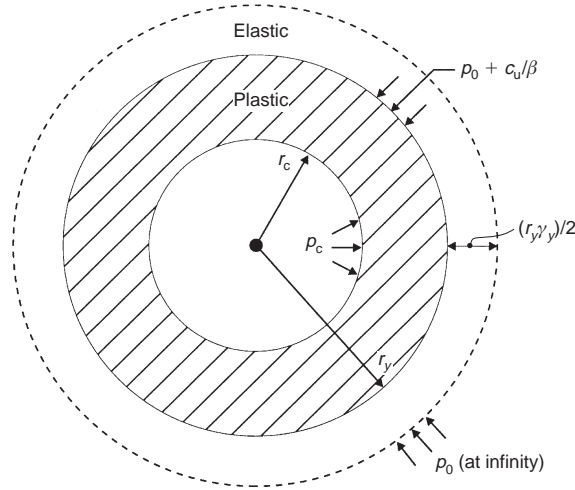


Fig. 4. Stress and radii for perfectly plastic loading

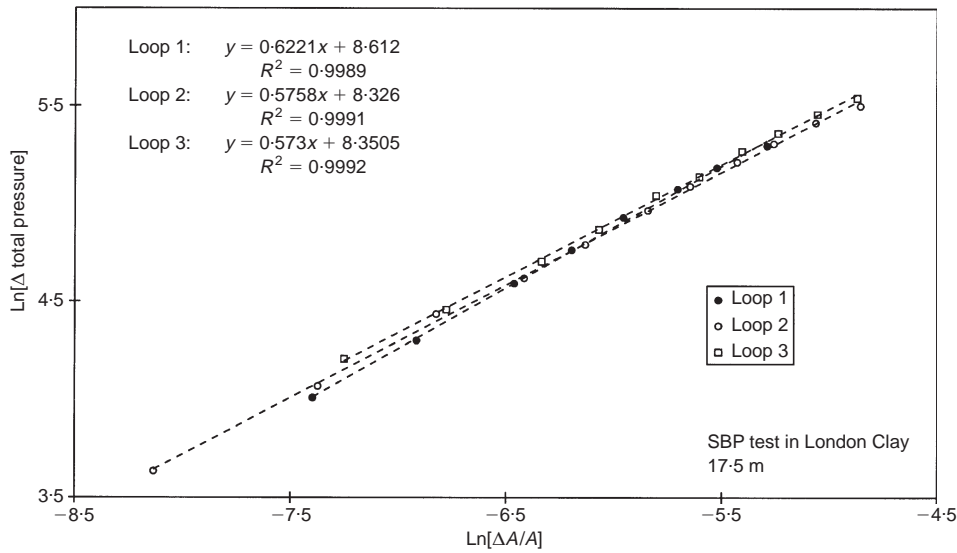


Fig. 5. Deriving the power law relationship from unload/reload cycles

and tangential shear modulus  $G_t$  by

$$G_t = \eta \beta^2 \gamma_c^{\beta-1} = \alpha \beta \gamma_c^{\beta-1} \tag{18}$$

For cycles conducted at the same mean effective stress, all data are expected to plot the same trend. There is some small scatter for this test, mostly confined to the first loop. This seems to be typical, with a more uniform response achieved when unloading from a well-developed plastic condition. These data suggest that the elastic exponent  $\beta$  is about 0.57.

DERIVING THE LIMITING ELASTIC SHEAR STRAIN

$\gamma_y$  For the purposes of deriving values for the undrained shear strength  $c_u$  and limit pressure  $p_{Limit}$  it is the perfectly plastic component of the solution that is utilized, and there is no difference in this respect between the simple elastic and non-linear elastic solutions.

Figure 6 shows the pressure and strain data from the test in Fig. 1 plotted in the form suggested by equation (15). In Fig. 6 the transition from elastic to plastic response is clear, the assumption of

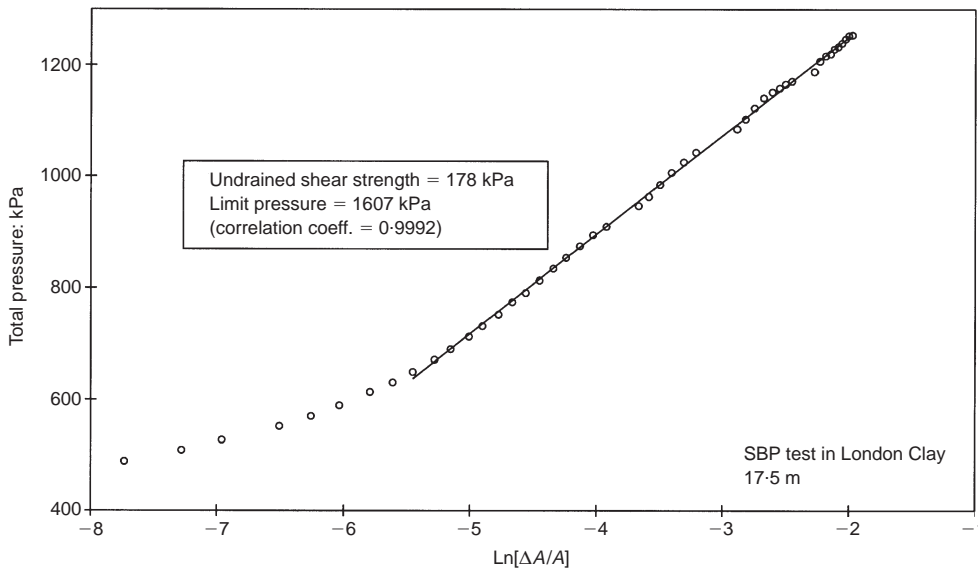


Fig. 6. Deriving the undrained shear strength and limit pressure

perfect plasticity seems reasonable and so the data from about 650 kPa onwards have been fitted by regression analysis. The correlation to a straight line is excellent, giving an undrained shear strength of 178 kPa and a limit pressure of 1607 kPa.

The significant advantage of applying the new analysis is the ability to give good predictions of the shear strain at which the material becomes fully plastic. To extract the yielding shear strain, equation (14) can be rearranged:

$$\gamma_y = \frac{c_u}{G_y} = \exp \left[ \left( \frac{p_{Limit} - p_0}{c_u} \right) - \left( \frac{1}{\beta} \right) \right]^{-1} \quad (19)$$

Equation (19) can now be applied to the results from the example test. In addition to the undrained shear strength and limit pressure, values for the *in situ* lateral stress and elastic response are required. For this test, inspection of the loading curve near lift-off suggests that 449 kPa would be a reasonable choice for  $p_0$  and from Fig. 5 a non-linear elastic exponent of 0.57 has been selected. The results for the example test are shown in Table 1, and are compared with the result that would be obtained for the linear elastic solution.

Table 1. Deriving the maximum elastic shear strain using equation (19). Input parameters (kPa):  $p_{limit} = 1607$ ,  $c_u = 178$ ,  $p_0 = 449$

| Elastic exponent | $G_y$ : MPa | $\gamma_y$ : % |
|------------------|-------------|----------------|
| $\beta = 0.57$   | 21.2        | 0.86           |
| $\beta = 1$      | 43.8        | 0.41           |

One method of showing that the non-linear elastic results are more applicable than the simple elastic solution is to plot the mobilized shear stress against shear strain directly. Provided the mode of deformation is plane strain shearing at constant specific volume, then Palmer (1972) shows the mobilized shear stress at any point can be obtained from the current slope of the loading curve. The result of applying the Palmer procedure to the example test is shown in Fig. 7. It is apparent that the simple elastic solution greatly underestimates the range of the elastic response, but the non-linear elastic solution is in good agreement with the rigorously correct but awkward to use Palmer analysis.

#### IMPLICATIONS OF THE NON-LINEAR ELASTIC SOLUTION

##### Tensile stresses

From equations (2) and (3) we can write

$$\sigma_r - \sigma_\theta = 2\tau = 2\alpha\gamma^\beta \quad (20)$$

At the cavity wall, equation (7) shows that

$$\sigma_r = p_0 + [\alpha/\beta]\gamma^\beta \quad (21)$$

hence

$$\sigma_\theta = p_0 - \alpha[2 - 1/\beta]\gamma^\beta \quad (22)$$

However, if as the example test shows,  $\beta$  takes a value of about 0.5 then  $\sigma_\theta \approx p_0$ , and will remain so until the material becomes fully plastic. If the circumferential stress cannot reduce, then tensile stresses cannot be generated. The possibility of

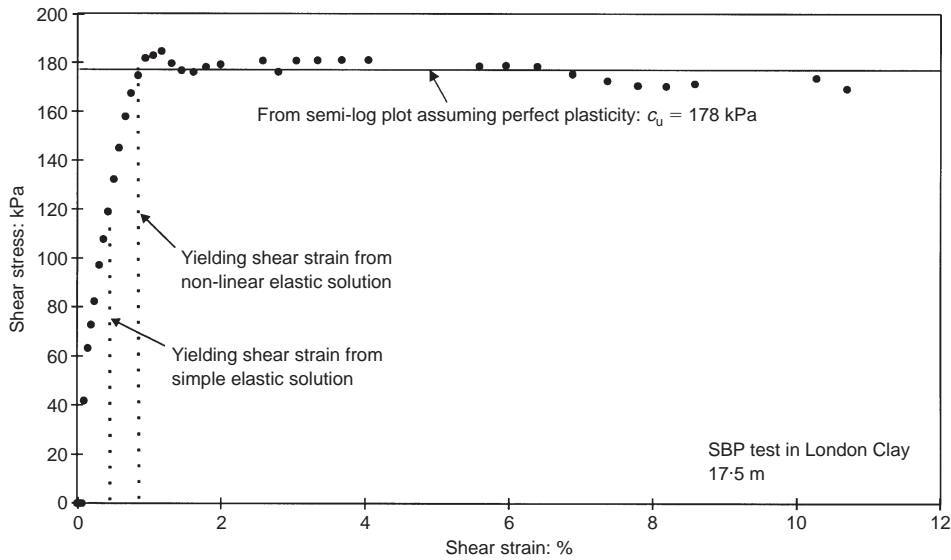


Fig. 7. Inspecting the strain required to reach the fully plastic condition

cracking emerges as a characteristic of linear elasticity, more appropriate for rock.

*Excess pore water pressure*

Because of the non-linearity of the stress–strain curve, the mean normal stress increases during the elastic phase of the loading, and does not remain constant as it would for an ideally elastic material.

Figure 8 sketches the relationships between the major and minor stresses, and from this it follows that the change in mean normal stress is given by

$$\Delta \frac{1}{2}(\sigma_1 + \sigma_3) = \frac{1}{2}(\Delta p + \Delta p(1 - 2\beta)) = (1 - \beta)\Delta p \tag{23}$$

The simplest view of non-linear elasticity in an isotropic soil is that constant bulk modulus links volume change to change in mean effective stress.

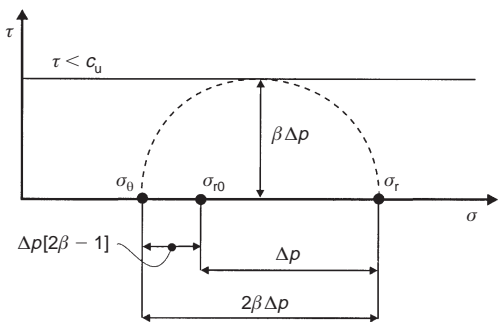


Fig. 8. Elastic stress distribution

This is consistent with a micromechanical action whereby particles are flattened at their points of contact due to the normal effective stress  $\sigma'$  irrespective of whether these contacts are sliding or not. If this description is accepted, then non-linear elastic deformations occur at constant mean effective stress if they are at constant volume.

More complex mechanisms for pore pressure generation may be imagined, but adopting the assumption of constant mean effective stress during non-linear elastic shearing implies that the pore pressure  $u$  will be

$$u = u_0 + (1 - \beta)\Delta p \tag{24}$$

The relationship between effective and total stress paths is sketched in Fig. 9, and the changing pore pressure versus changing total pressure in Fig. 10.

By extracting the total stress at yield from equation (13) an expression for the pore water pressure generated during the plastic phase of the test is given:

$$u = c_u [\ln(\gamma_c) - \ln(\gamma_y)] \tag{25}$$

The complete expression for the pore water generated during an undrained cavity expansion is obtained by combining equation (24) with equation (25):

$$u = u_0 + c_u \left[ \left( \frac{1 - \beta}{\beta} \right) + \ln(\gamma_c) - \ln(\gamma_y) \right] \tag{26}$$

This result although speculative would explain why SBP tests in clay invariably show excess pore water pressures being generated during the initial elastic loading phase. Unfortunately, field data usually in-

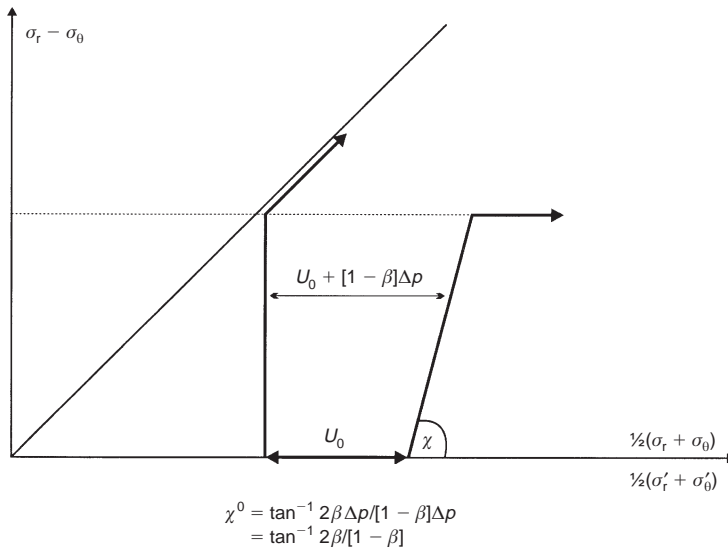


Fig. 9. Total and effective stress paths

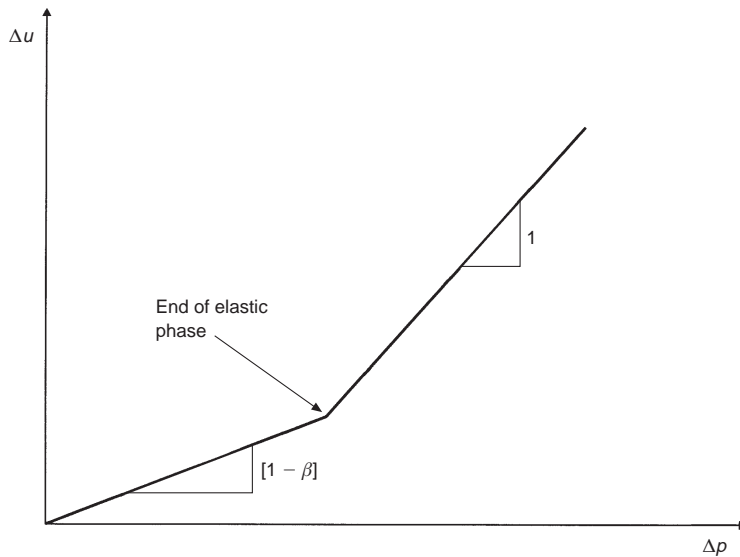


Fig. 10. Excess pore pressure versus total pressure

dicating some excess pore water pressure is also caused by the insertion of the instrument, and this disturbance masks the true elastic response. The measured pore water pressure data for two tests are plotted in Fig. 11. The results for the example test at 17.5 m are not convincing, but data from a shallower test in the same borehole fit the predicted behaviour shown in Fig. 10 almost exactly. Potentially these data give another means for identifying the cavity reference pressure  $p_0$ , yield stress  $p_y$  and  $\beta$ .

*Inappropriate use of a simple elastic solution to a non-linear elastic problem*

In general, applying a linear elastic analysis to a non-linear elastic problem will underestimate the elastic contribution. Any calculation based on the Gibson & Anderson solution apart from the determination of undrained shear strength and limit pressure is affected. Analyses attempting to force the entire pressuremeter curve to fit a simple elastic/perfectly plastic model are most vulnerable to error.

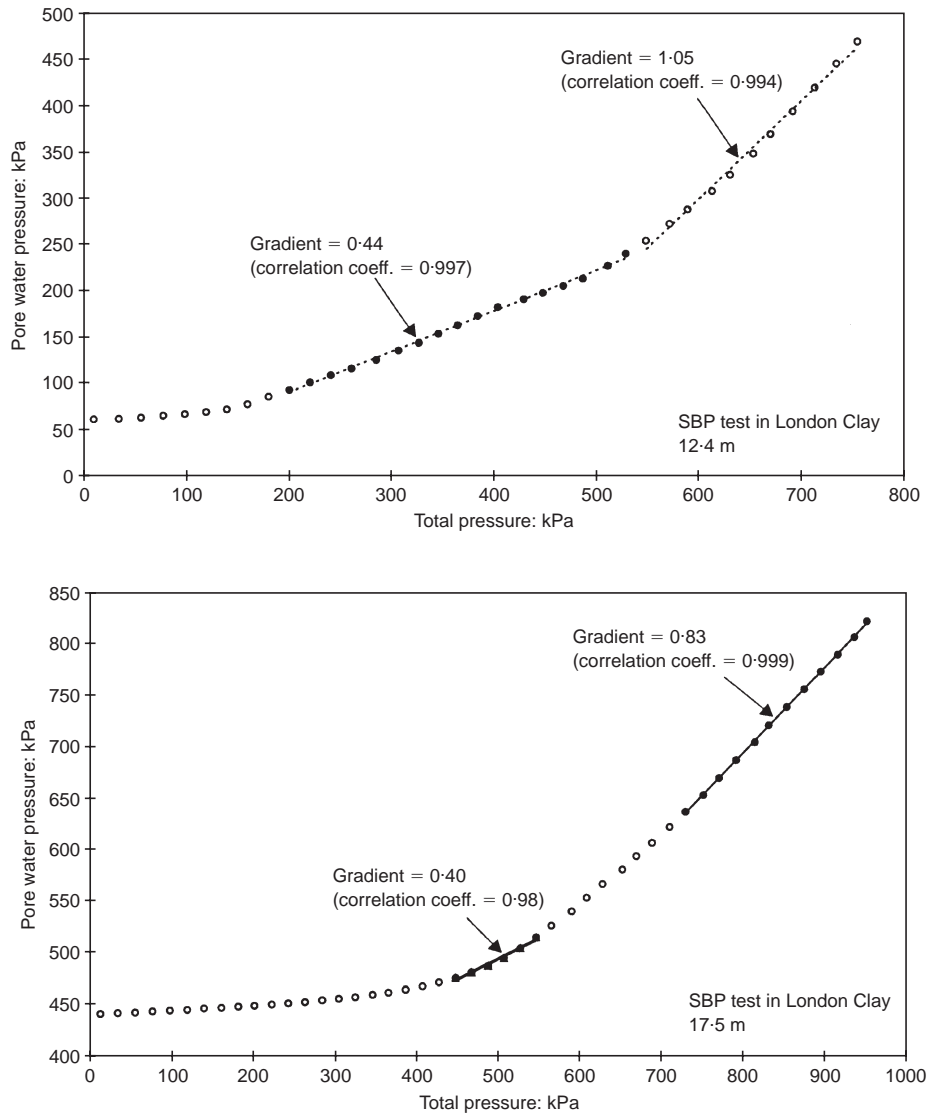


Fig. 11. Two examples from the same borehole of pore water pressure plotted against total pressure

An interesting example of this is the Houlby & Withers (1988) solution for the special case of a pressuremeter unloading from the limit pressure. This solution is frequently used to derive values for undrained shear strength, modulus and *in situ* horizontal stress for a cone pressuremeter test in clay. Essentially this analysis solves equation (14) but with simple elastic material assumed so the elasticity exponent  $\beta$  is set to 1. If  $\beta$  is about 0.5, then the *in situ* horizontal stress will be overestimated by a stress equal to the undrained shear strength. This finding is consistent with results from tests in the field reported by Houlby & Withers.

#### CONCLUSIONS

A closed form solution for the undrained cavity expansion in a non-linear elastic perfectly plastic soil has been given. The main points are repeated here:

- The non-linear elastic response of soils with the characteristic that stiffness reduces with strain can be described by a power law of the form  $\tau = \alpha\gamma^\beta$ .
- While the material is responding elastically, pressure and shear strain at the cavity wall are related by



$$p_c - p_0 = \frac{\alpha}{\beta} \left( \frac{\delta A}{A} \right)^\beta$$

- (c) Thereafter, the assumption of perfect plasticity and undrained expansion leads to

$$p_c = p_0 + c_u \left[ \frac{1}{\beta} - \ln(\gamma_y) + \ln(\gamma_c) \right]$$

- (d) Pore water generated during the loading is given by

$$u = u_0 + c_u \left[ \left( \frac{1 - \beta}{\beta} \right) + \ln(\gamma_c) - \ln(\gamma_y) \right]$$

- (e) These equations reduce to well-known expressions for simple elastic/perfectly plastic undrained cavity expansion if  $\beta$  is set to 1.

- (f) Undrained shear strength and limit pressure are derived in the usual way from the gradient and intercept of a plot of total pressure versus the natural log of current shear strain.

- (g) Unload/reload loops if replotted on log-log scales using the turn-around point in the cycle as an origin give a linear plot with gradient  $\beta$  and intercept  $\ln[\alpha/\beta]$ .

- (h) Secant shear modulus is given by  $G_s = \alpha\gamma_c^{\beta-1}$ .

- (i) Tangential shear modulus is given by  $G_t = \alpha\beta\gamma_c^{\beta-1}$ .

The new solution shows that the application of a simple elastic analysis to non-linear elastic problem will give a completely misleading picture of the distribution of stresses and strains.

#### NOTATION

|                    |   |
|--------------------|---|
| $c_u$              | undrained shear strength  |
| $G$                | shear modulus, the suffix s or t denoting secant or tangential    |
| $G_y$              | shear modulus at elastic strain $\gamma_y$                        |
| $p_c$              | pressure applied to cavity wall                                   |
| $p_{\text{limit}}$ | limit pressure at which indefinite expansion of the cavity occurs |

|              |  |
|--------------|--|
| $p_y$        | pressure at cavity wall at onset of fully plastic behaviour  |
| $p_0$        | cavity reference pressure, being the <i>in situ</i> horizontal stress for the ideal test   |
| $r$          | radius, with the suffix c denoting radius of the cavity wall   |
| $u$          | pore water pressure, $u_0$ being ambient pore water pressure   |
| $\alpha$     | stiffness constant   |
| $\beta$      | exponent of elasticity, where 1 is linear elastic  |
| $\gamma_c$   | shear strain at cavity wall  |
| $\gamma_y$   | shear strain at onset of fully plastic behaviour   |
| $\Delta A/A$ | constant area ratio, obtained from cavity strain via $1 - 1/(1 + \epsilon_c)^2$  |
| $\epsilon$   | strain, usually carrying the suffix a, r or $\theta$ for axial, radial or circumferential strain   |
| $\epsilon_c$ | circumferential strain at borehole wall  |
| $\eta$       | intercept on log-log plot of $\Delta p_c$ versus $\Delta \gamma_c$ —equal to $\alpha/\beta$  |
| $\rho$       | a small radial displacement  |
| $\sigma$     | stress, usually carrying the suffix r or $\theta$ to distinguish between radial and circumferential stress. A prime denotes effective stress |
| $\tau$       | shear stress, suffix c denoting shear stress at cavity wall  |

#### REFERENCES

- Bolton, M. D., Sun, H. W. & Britto, A. M. (1993). Finite element analyses of bridge abutments of firm clay. *Comput. Geotech.* **15**, 221–245.
- Gibson, R. E. & Anderson, W. F. (1961). In situ measurement of soil properties with the pressuremeter. *Civil Engng Public Works Rev.* **56**, No. 658, 615–618.
- Gunn, M. J. (1992). The prediction of surface settlement profiles due to tunnelling. *Predictive soil mechanics, Proceedings of the Wroth Memorial Symposium, Oxford*, pp. 304–316.
- Houlsby, G. T. & Withers, N. J. (1988). Analysis of cone pressuremeter test in clay 1988. *Géotechnique* **38**, No. 4, 575–587.
- Palmer, A. C. (1972). Undrained plane-strain expansion of a cylindrical cavity in clay: a simple interpretation of the pressuremeter test. *Géotechnique* **22**, No. 3, 451–457.